ELSEVIER

Polymer 43 (2002) 881–889

polymer

www.elsevier.com/locate/polymer

Rheological behavior of cellulose/monohydrate of *N*-methylmorpholine *N*-oxide solutions. Part 2. Glass transition domain

J.-F. Blachot[a], L. Chazeau[b,*], J.-Y. Cavaille[b]

[a]*CERMAV-CNRS, Université J. Fourier, BP 53X, 38041 Grenoble Cedex, France*
[b]*GEMPPM, UMR CNRS-INSA#5510, INSA de Lyon, 69621 Villeurbanne Cedex, France*

Received 15 May 2001; received in revised form 10 September 2001; accepted 13 September 2001

Abstract

Dynamic mechanical experiments performed with original conditions allowed the analysis of a solution containing 15% cellulose dissolved in a monohydrate of *N*-methylmorpholine *N*-oxide (NMMO) in the amorphous state. The glass transition zone is studied by dynamic tensile experiments, while dynamic torsion technique is used to determine the viscoelastic behavior in the glassy state. A master curve of the storage and loss modulus versus frequency can be deduced from the isochronal curves measured by both techniques. This work allows one to complete the corresponding master curve obtained for the 'liquid' state and presented in a previous work [Rheol. Acta 1998;37: 107]. The measurements below the glass transition temperature exhibit two secondary relaxations. A modeling of the overall viscoelastic behavior, using the Nowick and Berry approach and the quasi-point defect theory, is proposed. Physical parameters deduced from this modeling are then discussed. © 2001 Published by Elsevier Science Ltd.

Keywords: Cellulose; Modeling; Viscoelasticity

1. Introduction

Cellulose is not a thermoplastic polymer, its processing requires either a homogeneous chemical modification (viscose process) or its dissolution in a true solvent [1]. In fact, one issue is to replace the viscose process, known to be polluting, by a simple dissolution of cellulose in solvent like *N*-methylmorpholine *N*-oxide (NMMO). As a matter of interest of such an alternative, the generic name 'Lyocell' is now given to such cellulose fibers directly produced from a solution. Production of Lyocell fibers from cellulose/NMMO–H_2O started a few years ago [2]. Gagnaire et al. [3] have demonstrated that the cellulose/(NMMO–H_2O) system forms a true solution, i.e. it is homogeneous at the molecular level.

Our previous work [4] described the mechanical properties in the 'liquid' state (viscous flow and rubbery plateau) of cellulose dissolved in monohydrate of NMMO in the concentrated isotropic regime. Thus, this study, dealing with the effect of concentration and molecular weight also, was quite relevant from the application point of view, more precisely for textile purpose, as the use of these solutions increases to replace the viscose process. From a more fundamental point of view, it is interesting to complete this study for lower temperatures since the studies of glassy systems with low concentration of polymer are rare. This last part of a series of two papers devoted to the study of the rheology of a solution containing 15% w/w of cellulose dissolved in a monohydrate of NMMO investigates the glass transition zone and the main part of the glassy state. A modeling of the viscoelastic behavior is then proposed and discussed.

2. Experiments

2.1. Preparation of the solution

The solution contained 15% (w/w) of cellulose, with an average degree of polymerization (DP) equal to 600 (determined from viscosimetric measurements). First, cellulose was mixed with hydrated NMMO from Texaco with a water content of 40% determined by refractometry. Then, 0.1% (w/w) of propylgallate was added as an antioxidant to prevent cellulose degradation. The resulting slurry was

* Corresponding author. Address: GEMPPM, INSA de Lyon, 69621 Villeurbanne Cedex, France. Tel.: +33-4-72-43-61-30; fax: +33-4-72-43-85-28.

E-mail address: laurent.chazeau@insa-lyon.fr (L. Chazeau).

0032-3861/02/$ - see front matter © 2001 Published by Elsevier Science Ltd.
PII: S0032-3861(01)00631-0

stirred in a mixing device (IKA-Laboratory Kneader HKD-T0.6) and the excess of water was removed under vacuum at increasing temperature (up to 105°C). After 1.5 h, a homogeneous solution, as observed by optical microscopy, was obtained. The average DP was found to be unaffected by these treatments.

2.2. Samples preparation

A mould, with dimensions (mm) $50 \times 12 \times 1.2$, was filled with granules of solution which were melt at 100°C for 10 min to eliminate all the seeds of crystallization. This manipulation was performed under vacuum. The mould was then pressed under 50 bars for 30 s, and quenched in a liquid nitrogen bath. Then, the sample was quickly removed from the mould and cut as parallelepiped (mm) $50 \times 6 \times 1.2$ at a temperature slightly higher than the glass transition temperature (T_g). Later, the samples were slowly cooled and stored in a liquid nitrogen bath. It was checked by differential scanning calorimetry (DSC) that the samples were totally amorphous and the glass transition was found at 242 K (measurements performed with a 10 K/min heating rate).

2.3. Measurements

The main technique used in this study is the so-called dynamic mechanical analysis, where measurements are performed with the help of mechanical spectrometers. They provide complex modulus data versus frequency and/or temperature. For sensitivity reasons and range of temperature rate, the experiments are performed using two different apparatus.

The Mécanalyseur (METRAVIB S.A.). This apparatus is a mechanical spectrometer constituted by an inverted torsion pendulum working in the sub-resonant forced oscillations mode. It was developed at GEMPPM (INSA, LYON) and is commercialized by Metravib, S.A. [5]. It allows us to perform measurements, for frequencies between 10^{-5} and 1 Hz, of the dynamic modulus ($G^* = G' + iG''$) and internal friction ($\tan \phi = G''/G'$), where G' and G'' are the storage and the loss modulus, respectively. The maximum amplitude of deformation is around 10^{-5}. The raising temperature rate ranges from 13 to 120 K/h depending on the frequency of analysis.

The solid analyzer RSAII (Rheometrics). This setup works in the dynamic regime using tensile, compression or flexural mode. The experiments are performed using the tensile mode in the glass transition and the rubbery plateau domains. The apparatus allows measurements at frequencies ranging from 2×10^{-3} up to 20 Hz. The temperature control using an airflow allows faster temperature rates than with the Mécanalyseur. This dynamic tensile experiment determines the complex Young modulus E^* as a function of temperature. As cellulose solutions are homogeneous and thus isotropic, E^* can be converted into the corresponding values of the shear modulus G^* by

$$G^* \approx \frac{E^*}{2(1+\nu)} \tag{1}$$

where ν is the Poisson factor. In polymer, ν ranges from about 0.3 for the glassy state up to nearly 0.5 for the liquid state. This variation is negligible with regard to the modulus variation within this zone. An average value of ν equal to 0.4 is used and G^* is deduced from Eq. (1).

3. Results and discussion

3.1. Study of the glass transition zone

3.1.1. Isochronal curves

As described in Section 2, for the solution studied, monohydrate of NMMO starts to crystallize within half an hour for temperatures above 260 K. To avoid this phenomenon, the glass transition zone is first studied by dynamic tensile test in the 225–310 K temperature range, using the relatively high raising temperature rate of 5 K/min. This high rate is combined with a frequency of analysis of 1 Hz, which allows quick and suitable measurements. The strain amplitude is fixed at 0.01%, i.e. within the linear behavior domain.

The plots of the storage modulus G', the loss modulus G'' and the loss tangent are presented in Fig. 1. The as-recorded values of G' and G'' within the rubber plateau zone are higher than those obtained for the liquid state with the cone and plate geometry [1,6]. Since the conditions of preparation and setting of the sample does not allow any crystallization to occur, it is concluded that the gap observed between both curves is probably due to the use of different techniques. In fact, the determination of G' and G'' in the

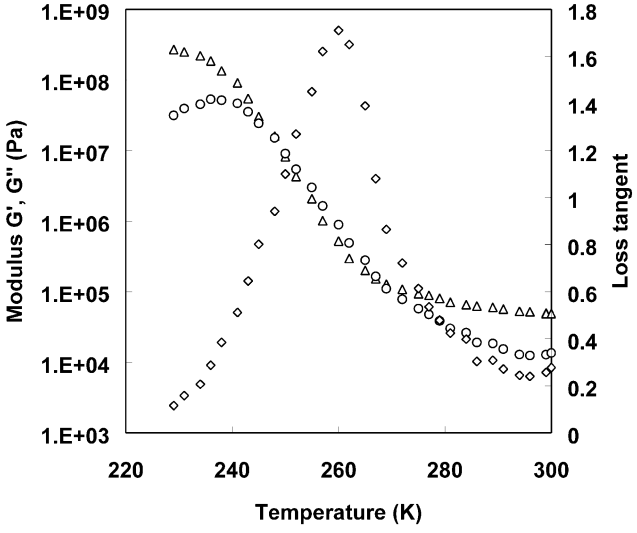

Fig. 1. Storage, loss modulus and loss tangent versus temperature for a 15% w/w cellulose/(NMMO–H_2O) solution. Dynamic tensile test performed at $f = 1$ Hz, G' (△), G'' (○), loss tangent (◇).

solid state requires the precise knowledge of the sample dimensions. On the contrary, the experiments performed using the cone and plate geometry do not present these uncertainties, and thus are taken as reference and all the other curves are vertically shifted with regard to them.

A second set of experiments is performed with the Mécanalyseur at two different frequencies, 1 and 10 Hz at a raising temperature rate slower than 5 K/min (Fig. 2). Therefore, to avoid any crystallization problem, the temperature range is reduced to 225–260 K. It is checked that the curve obtained at 1 Hz superimposes well with the curve of Fig. 1, previously obtained at higher heating rate. This confirms that crystallization effect can be neglected and also that the high temperature rate (5 K/min) does not lead to a shift due to thermal inertia.

Isothermal experiments are not suitable within the glass transition zone because as they require long time, possible crystallization can occur. However, one can deduce the graph of the modulus data versus frequency from the isochronal measurements obtained in the glass transition zone, as discussed. For this purpose, a determination of the evolution of the shift factor versus temperature is needed.

3.1.2. Determination of the shift factor a_T temperature dependence

The temperature shifts in the glass transition domain are deduced from both G' and G'' isochronal measurements performed at 1 and 10 Hz (cf. Fig. 2). Though it is well known that the relaxation time temperature dependence does not follow a simple Arrhenius law, within a small temperature range, one can write

$$\tau = \tau_0 \exp\left(\frac{E_a}{RT}\right) \tag{2}$$

where τ_0 and E_a are just phenomenological parameters (E_a is the so-called apparent activation energy). Consequently, from the values of the temperature shifts ΔT corresponding to a frequency change by a factor (a_T) of 10, one can approximate E_a from

$$\ln(10) = \frac{E_a(T)}{R}\left(\frac{1}{T} - \frac{1}{T+\Delta T}\right) \tag{3}$$

The apparent activation energies obtained from Eq. (3) are plotted in Fig. 3. From these values, the relative values of a_T as a function of temperature are calculated from the segmental reconstruction of their curve, as shown in Fig. 4. This leads to the equation

$$\begin{aligned}\ln[a(T)] - \ln[a(T+5)] &= \frac{E_a(T)}{R}\left\{\frac{1}{T} - \frac{1}{2}\left(\frac{1}{T} + \frac{1}{T+5}\right)\right\} \\ &+ \frac{E_a(T+5)}{R}\left\{\frac{1}{T} - \frac{1}{2}\left(\frac{1}{T} + \frac{1}{T+5}\right)\right\}\end{aligned} \tag{4}$$

Reaching this point, it is necessary to check if the data obtained from measurements performed in the liquid state and data obtained following the above-described procedure exhibit a reasonable continuity. One simple way to perform this verification is to use the well-known Williams, Landel and Ferry [7] (or WLF) equation and to plot all the set of

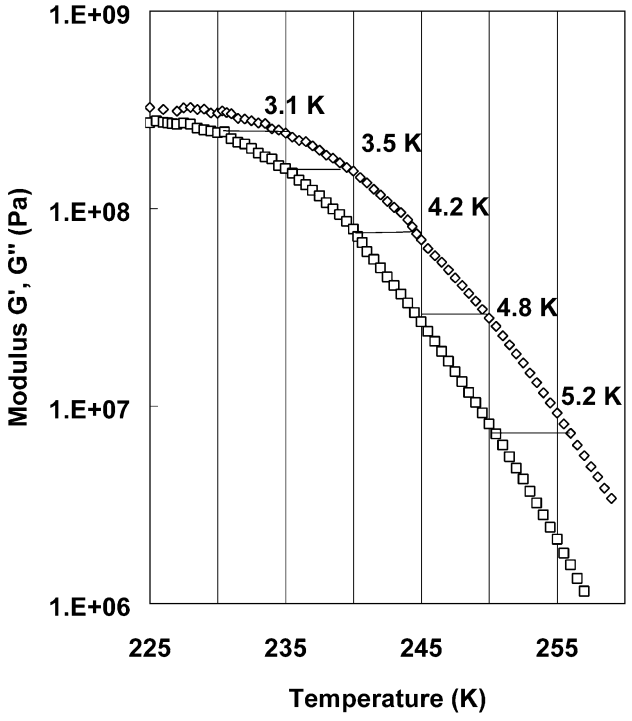

Fig. 2. Storage modulus G' versus temperature (dynamic torsion), obtained at 1 Hz (□), 10 Hz (◇) for a 15% w/w cellulose/(NMMO–H_2O) solution.

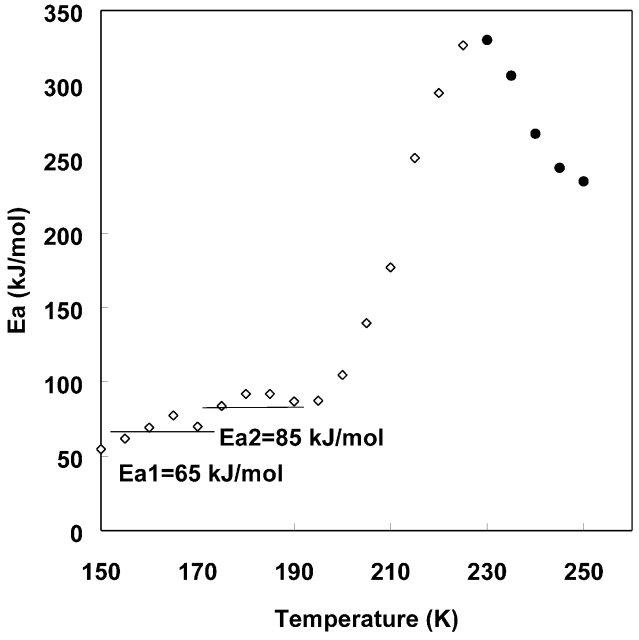

Fig. 3. Apparent activation energy versus temperature in the glassy state, from dynamic torsion tests (◇) and dynamic tensile tests (●).

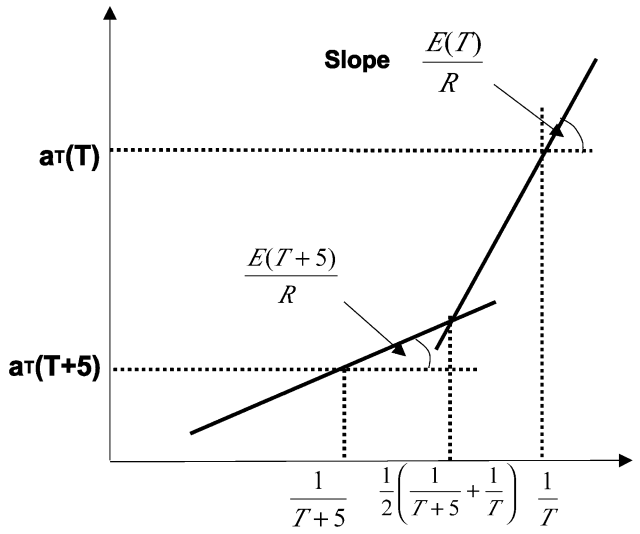

Fig. 4. Schematic representation of the segmental reconstruction of the a_T curve.

data in a unique figure. This model proposes the evolution of the shift factor as follows:

$$\log(a_T) = -\frac{C_1(T - T_g)}{C_2 + (T - T_g)} \tag{5}$$

which can also be written as

$$\frac{T - T_g}{\log(a_T)} = -\frac{1}{C_1}(T - T_g) - \frac{C_2}{C_1} \tag{6}$$

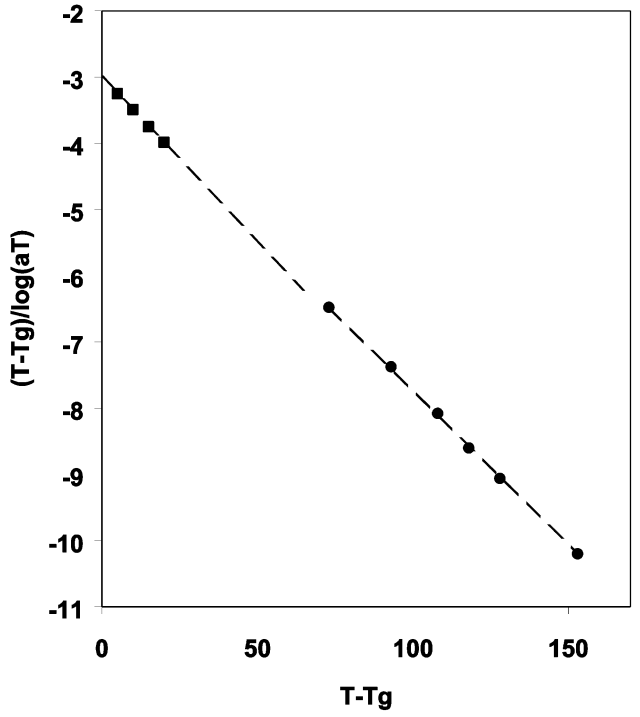

Fig. 5. $(T - T_g)/\log(a_T)$ versus $(T - T_g)$: experimental data from dynamic tensile tests (■) and from cone–plate measurements (●), and WLF equation (– – –).

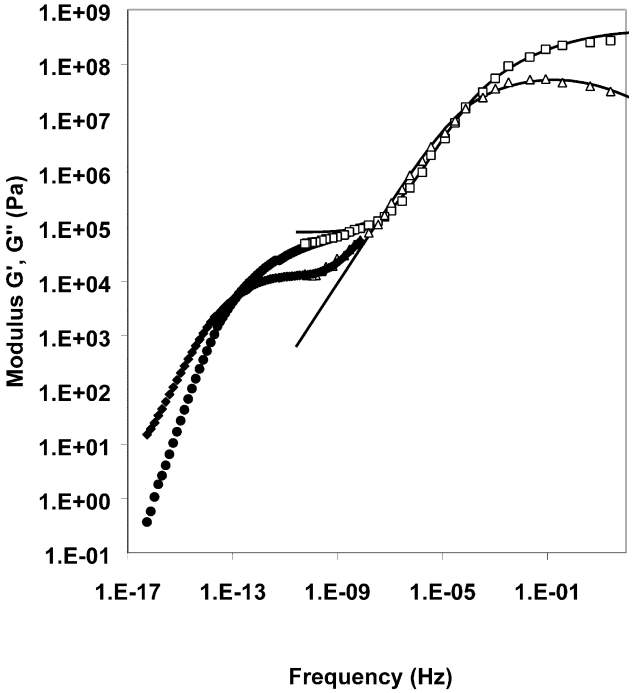

Fig. 6. Master curves of G' (□ and ◆) and G'' (△ and ●) versus frequency, reduced to $T = 235$ K, obtained by superimposition of the data from cone and plate (black marks) and from dynamic tension (open marks) experiments. Calculated curve (bold line).

This means that the data checking this equation form a straight line plotting $(T - T_g)/\log(a_T)$ versus $T - T_g$. It is worthwhile to note that the plot of the shift factors measured during the study of the 'liquid state' of the solution, using the cone and plate geometry, and those deduced from the dynamic tensile test lead to a unique straight line (see Fig. 5). Though it is not a proof of the validity of our method, the above result is an indication that this procedure can be used to relate isochronal and isothermal data. However, the WLF equation does not lead to any conclusion about the relationship between the molecular mobility and the viscoelastic behavior. For this reason, we will use a different approach to go further.

From the knowledge of these data, one can represent on the same graph the isothermal data obtained during the study of the 'liquid state' and the isochronal ones describing the glass transition zone. Figs. 6 and 7 show the plot of the master curve of G', G'' and the plot of loss tangent, respectively, versus frequency, reduced to $T = 230$ K, on a large frequency domain $[10^{-6}, 10^{5}]$. The good superimposition of the tan ϕ values, which does not depend on the dimensions of the samples, demonstrates the suitability of the method.

3.2. Study of the glassy state

3.2.1. Isochronal curves

Fig. 8 represents the modulus and loss tangent curves obtained using dynamic torsion technique at two frequencies, 1 and 0.1 Hz. The measurements were performed over

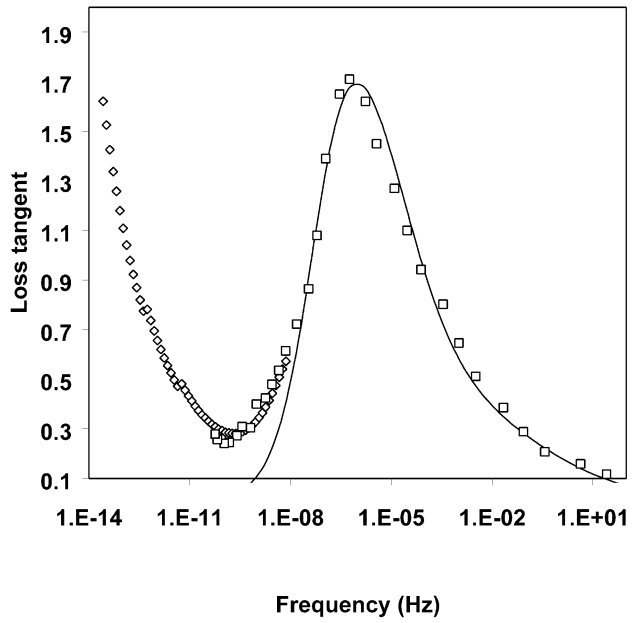

Fig. 7. Master curve of tan ϕ versus frequency, reduced to $T = 235$ K, obtained by superimposition of the data from cone and plate (◇) and from dynamic tension (□) experiments. Calculated curve (bold line).

a temperature range of 150–235 K. The sample was not subjected to any aging before measurements. The setting of the sample inside the spectrometer induces a stay at temperatures above T_g for few minutes, which could lead to a slight crystallization. But one can notice in Fig. 9 that these curves superimpose well with those performed within the glass transition zone and measured by dynamic

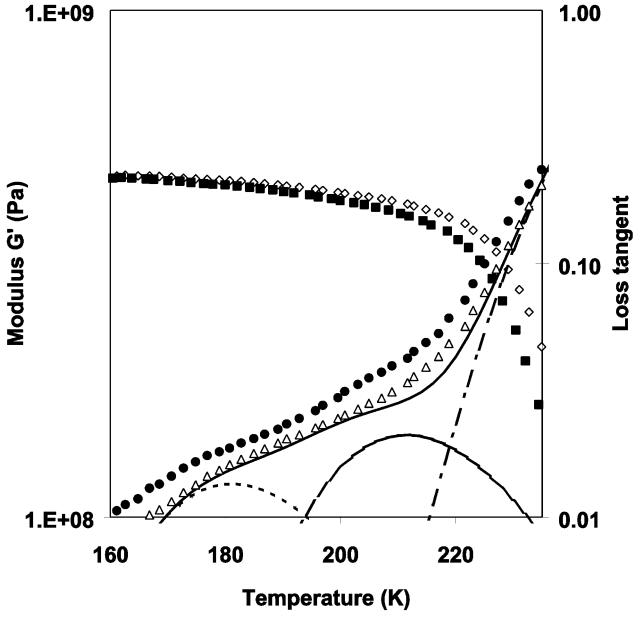

Fig. 8. Dynamic torsion analysis in the glassy state of cellulose (15% w/w)–(NMMO–H_2O) solution. G' (■ and ◇) and loss tangent (● and △) curves measured at 0.1 Hz (black marks) and 1 Hz (open marks). Calculated tan ϕ curves at 1 Hz for the γ relaxation (- - -), for the β relaxation (– – –), the α relaxation (–·–·–), and the serial coupling of the three relaxation (bold

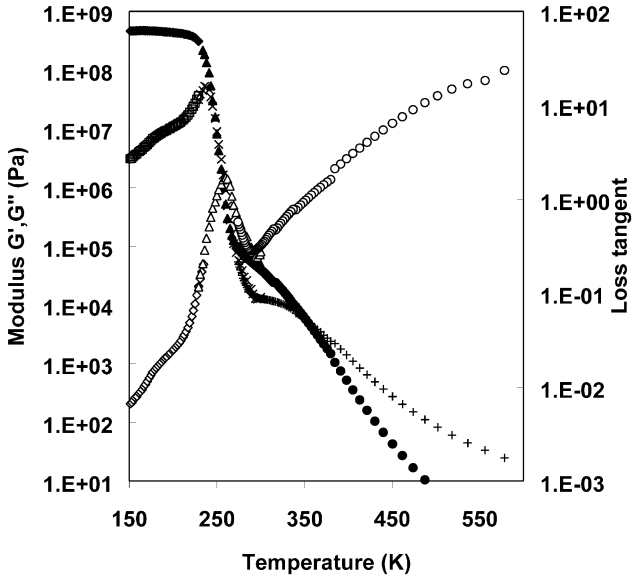

Fig. 9. G' (◆, ▲ and ●), G'' (□, × and +) and loss tangent (◇, △ and ○) versus temperature measured at 1 Hz: data from cone and plate, dynamic tension and dynamic torsion techniques.

tensile tests. Thus, it is possible to plot the behavior of cellulose/NMMO solution from the glassy state up to the viscous flow.

3.2.2. Evolution of the shift factor a_T versus T

As before, the evolution of both the shift factors and activation energy versus temperature are calculated from the temperature shifts measured between the two frequency data. Fig. 3 plots the deduced activation energy as a function of temperature. When G'' reaches its maximum, it is generally assumed that $\omega\tau = 1$, ω being the solicitation pulsation and τ the average value of the relaxation time for the considered temperature. The maximum of G'' is found at 235 K at 1 Hz (cf. Fig. 1). The temperature dependence of the relaxation time is plotted versus $1/T$ in Fig. 10. Though the sample was not subjected to any aging, the change in the slope observed around 230 K, i.e. 12 K below the glass transition temperature (found by DSC), is significant. This probably indicates an in situ aging of the sample occurring during the experiment, though the latter was performed at a heating rate of 35 K/h. One can assume that systems constituted by polymers in solution present a fast aging. This assumption is confirmed by studies on solutions of sugars [8]. The consequence of this aging is that the sample cannot be considered in an isoconfigurational state below the glass transition temperature. Consequently, it is impossible to estimate the value of the apparent activation energy of the α relaxation from Fig. 10. Besides, the overlap of β and α relaxations would lead to an important underestimation of this activation energy.

On the other hand, Fig. 3 exhibits two plateaus in the low temperature domain. This should correspond to two relaxations (hereafter called γ and β), also shown in Fig. 8. The γ

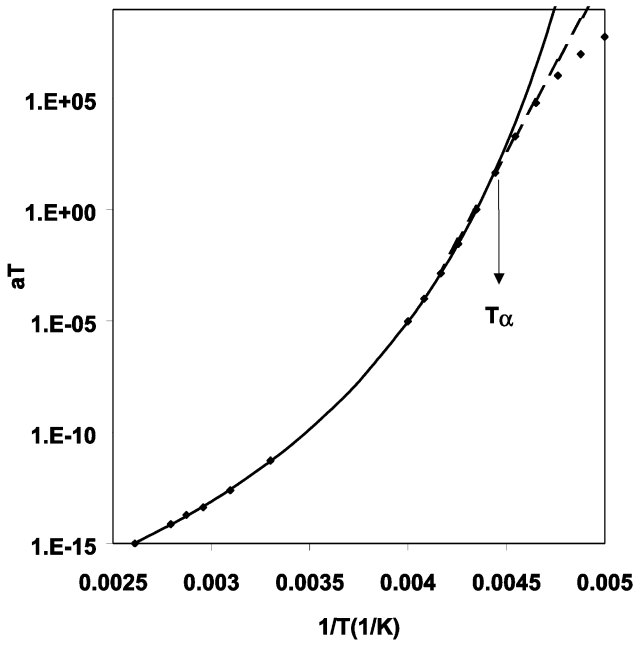

Fig. 10. Relaxation times versus temperature in the glass transition domain ◆. WLF model (bold line) and Arrhenius model with a 303 kJ/mol activation energy (dashed line).

relaxation has its G'' maximum for a frequency of 1 Hz at a temperature equal to 160 K. The β relaxation has its G'' maximum at about 200 K. They present apparent activation energies around 65 and 85 kJ/mol, respectively. These values are obtained from the temperature shift determined in the low temperature side of each G'' maximum, to avoid the two relaxation overlap effect. These two secondary relaxations might be induced by cellulose since this latter can present, in the presence of solvent, two relaxations in the same temperature domain, and with activation energy in the same range [9]. This point will be discussed later.

3.3. Modeling of the viscoelastic behavior

As usual, it will be considered that the macroscopic behavior results from the contribution of each relaxation processes. This means that the macroscopic strain (and hence, the compliance $[G^*_{\mathrm{tot}}(\omega)]^{-1}$) can be written as the sum of three contributions, as follows:

$$[G^*_{\mathrm{tot}}(\omega)]^{-1} = [G^*_{\gamma}(\omega)]^{-1} + [G^*_{\beta}(\omega)]^{-1} + [G^*_{\alpha}(\omega)]^{-1} \qquad (7)$$

We will now discuss how to evaluate each of these contributions.

3.3.1. Secondary relaxations

Following a theoretical approach described in the literature [10,11], the β relaxation spectrum can be fitted with a Gaussian distribution Ψ of relaxation time

$$\Psi\left(\ln\left(\frac{\tau}{\langle\tau\rangle}\right)\right) = \frac{1}{B\sqrt{\pi}}\exp\left[-\left(\frac{\ln\tau - \ln\langle\tau\rangle}{B}\right)^2\right] \qquad (8)$$

where B is the Gaussian distribution width; $\langle\tau\rangle$ is the most probable value of τ and corresponds to f_{m}, the frequency at the maximum of the G'' spectrum.

$$\langle\tau\rangle = \frac{1}{2\pi f_{\mathrm{m}}} = \tau_0 \exp\left(\frac{E}{RT}\right) \qquad (9)$$

where E is the average activation energy of the relaxation process and τ_0 is the pre-exponential factor.

It is then possible to model G^* by

$$G^*(\omega) = G_{\mathrm{R}} + (G_{\mathrm{U}} - G_{\mathrm{R}}) \times \int \frac{\mathrm{i}\omega\tau}{1+\mathrm{i}\omega\tau}\Psi\left(\ln\left(\frac{\tau}{\langle\tau\rangle}\right)\right)\mathrm{d}\ln\left(\frac{\tau}{\langle\tau\rangle}\right) \qquad (10)$$

which leads to

$$\frac{G'(\omega) - G_{\mathrm{R}}}{(G_{\mathrm{U}} - G_{\mathrm{R}})} = \int \frac{(\omega\tau)^2}{1+(\omega\tau)^2}\Psi\left(\ln\left(\frac{\tau}{\langle\tau\rangle}\right)\right)\mathrm{d}\ln\left(\frac{\tau}{\langle\tau\rangle}\right) \qquad (11)$$

$$\frac{G''(\omega)}{(G_{\mathrm{U}} - G_{\mathrm{R}})} = \int \frac{\omega\tau}{1+(\omega\tau)^2}\Psi\left(\ln\left(\frac{\tau}{\langle\tau\rangle}\right)\right)\mathrm{d}\ln\left(\frac{\tau}{\langle\tau\rangle}\right) \qquad (12)$$

where G_{U} and G_{R} are the unrelaxed and relaxed modulus values, respectively, for the relaxation considered.

The activation energy of each relaxation is determined from Fig. 3. The pre-exponential terms $\tau_{0\beta}$ and $\tau_{0\gamma}$ are deduced from both Eq. (9) and the temperature of the G'' shoulders (where $\omega\tau = 1$). The unrelaxed and relaxed modulus of the relaxation processes are determined from the G' curve. The remaining adjustable parameters are the widths of the Gaussian distribution of the relaxation times. They are obtained by fitting the experimental data in Eq. (12).

3.3.2. α Relaxation

The α relaxation is analyzed with the help of a molecular model developed by Perez et al. [12–14]. Following this framework, on one hand, an amorphous material is characterized by density fluctuations (more generally speaking, entropy and enthalpy fluctuations) at the nanometric scale; mobility (local molecular motions) is larger where the local density (free enthalpy) is either maximum or minimum. On the other hand, the molecular diffusion processes are hierarchically correlated, i.e. at temperature around T_{g}, translational molecular motions require those very local and short motions to occur, which in turn allow more complex motions, and so on. Most of the time, these local motions are responsible for the secondary β relaxation. The main idea is that local shears occur (forming shear microdomains) under the application of a local shear stress and expand by hierarchical diffusion process to coalesce (which provides an irreversible or plastic strain contribution). Thus, this model provides in fact two main relationships, namely, the temperature and microstructure dependence of the average relaxation time for the α process, and the viscoelastic (complex) shear modulus as a function of both temperature and frequency.

Table 1
Parameters of the description of the α relaxation

Symbols	$G_{el} = G_{R\beta}$ (GPa)	Q	G_c (Pa)	χ	χ'	t_0	a
Value	0.44	0.025	8×10^4	0.28	0.74	2.71×10^{-4}	0.0028

The temperature and microstructure dependence of the molecular mobility is given by

$$\tau_{mol} = t_0 \left(\frac{\tau_\beta}{t_0} \right)^{1/\chi} \tag{13}$$

where the correlation parameter χ lies between 0 and 1 and t_0 is a scaling parameter. The larger the χ, the less important is the correlation effect. For $\chi = 1$, all the movements have the same rate and occur independently from each other. Roughly speaking, χ plays the role of an order parameter which depends on temperature (and below T_g, on physical aging). Then, it has been shown that within some approximations, the complex shear modulus $G^*_\alpha(i\omega)$ can be simply written as [15]:

$$G^*_\alpha(\omega) = G_c + \frac{G_{el} - G_c}{1 + (i\omega\tau_\alpha)^{-\chi} + Q(i\omega\tau_\alpha)^{-\chi'}} \tag{14}$$

with

$$\tau_\alpha = \left(\frac{\chi' Q}{\chi} \right)^{\frac{1}{(\chi' - \chi)}} \tau_{mol} \tag{15}$$

with τ_α, the relaxation time for the α relaxation, G_c the rubber modulus and G_{el} the unrelaxed modulus of the α relaxation (which in turn is the relaxed modulus of the β relaxation). Q depends on the amplitude of the relaxation. χ' accounts for both the obstacles limiting the local shear expansion, and the distribution of entanglements or cross-link nodes within the polymer [16,17]. χ' is 1 for molecular glasses, close to 1 for regular linear polymers, and decreases for random copolymers, semicrystalline polymers and thermosets. τ_α is proportional to τ_{mol} (Eq. (13)).

3.3.3. Isothermal data

Starting from experimental data, τ_α is identified with the experimental relaxation time. χ and χ' are deduced from the fit of the G' and G'' master curves ($T_{ref} = 235$ K) in the high frequency and the low frequency domain of the α relaxation, respectively. Q is deduced from the same fit. t_0 is then deduced from Eqs. (13) and (15). Corresponding parameters determined to describe the α relaxation are given in Table 1. The curve fits are satisfying and plotted in Figs. 6 and 7 for G' and G'', and tan ϕ, respectively.

χ is found to be equal to 0.28, which is the value also found for polystyrene and poly(methyl methacrylate), and for other usual polymers [18]. An estimation of the apparent activation energy of α relaxation below T_g can be derived from Eq. (13), replacing τ_β by its Arrhenius expression

$$E_\alpha = \frac{E_\beta}{\chi} \tag{16}$$

E_α is found to be equal to 303 kJ/mol, close to what is obtained for classical polymers. χ' is equal to 0.74. This value has to be compared with the value of 0.6 for poly(vinyl-chloride) [19], 0.76 for poly(methyl-butyl acrylate) [20], 0.83 for poly(methyl-methacrylate) and 1 for maltitol and sorbitol. In these cases, the more heterogeneous (at a submicron scale) the materials, the lower is χ'. For this reason, one could have expected a value close to 1 since the main constituent of the material studied is a solvent (85% by weight). The low value observed is equivalent to a large distribution of the viscoplastic relaxation times. This might be due to the large polymolecularity of cellulose [1], and/or to concentration heterogeneity in the materials [14]. One must also consider that the cellulose chain without the solvent presence is highly rigid in this temperature domain, leading to a more difficult expansion of the sheared micro-domains. The t_0 parameter is found to be equal to 2.7×10^{-4} s, which is comparable to the value of poly(methyl-butyl acrylate) (6.5×10^{-4} s) and much higher than the value found for poly(methyl-methacrylate) (10^{-16} s). Roughly speaking, the higher this parameter, the more important are the fast events compared to the slow ones involved in the movement of molecular segments. In the present case, the high t_0 value might be due to the effect of movements of solvent molecule in the cooperative process involved in the relaxation mechanism.

3.3.4. Isochronal data

The modeling approach is also used to describe the isochronal curves of Figs. 11 and 12. Above T_g, the variation of χ with temperature must be taken into account, which is, for amorphous polymers, at the origin of the usual WLF like behavior. For $T > T_g$, χ increases as the increase of disorder with temperature leads to a less cooperative molecular diffusion (its amplitude and/or its correlation distance decreases) [21]. For the sake of simplicity, χ is assumed to follow [12]:

$$\chi(T) \cong \chi(T_g) + a(T - T_g) \tag{17}$$

where $\chi(T_g)$ is equal to 0.28. a is adjusted from the fit of the relaxation times with Eq. (1) (cf. Fig. 10).

Figs. 8, 11 and 12 show the curve fits performed so that G' and G'' and therefore tan ϕ, be well described by G^*_{tot}. This needs a slight adjustment of the pre-exponential times

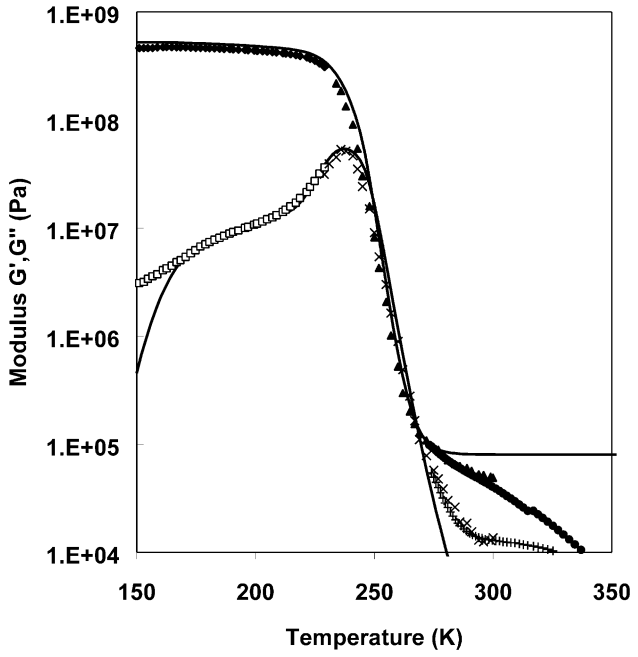

Fig. 11. Modeling (bold line) of the shear modulus G' versus temperature for a frequency of 1 Hz (same legend as Fig. 9).

of the secondary relaxations previously calculated from the G'' maxima. The corresponding parameters for both relaxations are given in Tables 2 and 3. The pre-exponential factor and the activation energy of the β relaxation are very close to those of literature for the β relaxation of cellulose in the presence of a low amount of water [9]. The value of the pre-exponential time is often discussed in terms of activation entropy. The lower the pre-exponential

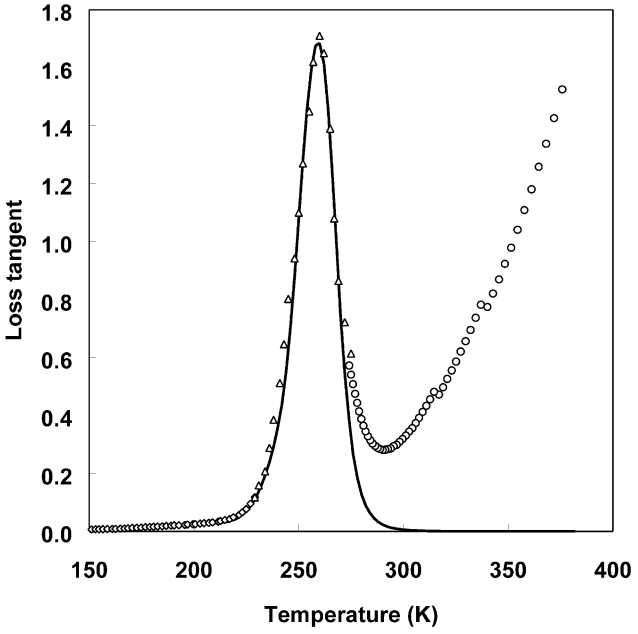

Fig. 12. Modeling (bold line) of the loss tangent versus temperature for a frequency of 1 Hz (same legend as Fig. 9).

Table 2
Parameters of the description of the γ relaxation

Symbols	E_γ (kJ)	τ_0 (s)	B_γ	$G_{U\gamma}$ (GPa)	$G_{R\gamma}$ (GPa)
Values	65	4×10^{-20}	4	0.525	0.49

time in the Arrhenius equation, the higher the activation entropy and the higher the cooperativity of the corresponding molecular motions [22]. Here, the small value (10^{-22} compared with 10^{-15} for PVC) might be due to the large cooperativity of the rotational movement of few units of the cellulose main chain. It is noticeable that the amount of water in the NMMO solution is much higher than few percent, which should lead to an activation energy below 70 kJ/mol. But it is also possible that the interaction between NMMO molecules and cellulose leads to more difficult movement of the main chain below the glass transition temperature, in the same way that DOP molecules leads to an increase of the β relaxation activation energy in PVC [23].

The γ relaxation observed is more difficult to identify. The activation energy value is higher than that of cellulose (65 kJ/mol against 42 kJ/mol) [9]. Moreover, the pre-exponential time is much lower, 4×10^{-20} s against about 10^{-12} s for cellulose, meaning a much higher cooperativity. This could also be due to the solvent presence, which might have strong interactions with the methylol groups possibly involved in the relaxation process.

Further discussions about the origin of these relaxations would need more experiments on cellulose–NMMO solution, with different concentrations. However, such a work was not in the frame of this study. Moreover, the technical problems met with the solution of this study, with a cellulose concentration of 15%, and the unsuccessful attempt made with lower cellulose concentration, suggest that it might be extremely difficult to perform mechanical tests in the glass transition domain with lower cellulose concentration.

The 'qpd' model used is a very powerful tool to describe the viscoelastic behavior of such material in the glass transition domain. Indeed, the theoretical curves obtained using Eq. (14) are in very good agreement with the experimental ones. Here, it suggests that the α relaxation observed is the manifestation of hierarchically correlated elementary movements of cellulose chain, though the concentration of the latter in the solution is relatively low (15% by weight). In particular, the chemical structure of cellulose chain might be responsible for the apparently large distribution of the viscoplastic relaxation time.

Table 3
Parameters of the description of the β relaxation

Symbols	E_β (kJ)	τ_0 (s)	B_β	$G_{U\beta}$ (GPa)	G_R (GPa)
Values	85	2×10^{-22}	4	0.49	0.44

4. Conclusion

The dynamic mechanical properties of a solution of cellulose dissolved in a monohydrate of NMMO, were analyzed in the glassy state and in the glass transition domain. It is noteworthy that pure NMMO crystallizes very easily but the dissolution of a small amount of cellulose drastically decreases the crystallization kinetics. Thus, it was checked that the kinetic of crystallization of 15% w/w cellulose/NMMO solution is slow enough to allow measurement in the amorphous state. The methodology proposed allows the reconstruction of the G' and G'' master curves versus frequency and the plot of the relaxation times versus temperature from only two isochronal measurements. This method appears to be well suited to the study of such materials, which presents important experimental difficulties.

The experimental data show the presence of two secondary relaxations which are attributed to cellulose but whose characteristics, determined through the Nowick and Berry approach [10,11], are influenced by the strong interactions between cellulose and NMMO (interaction at the origin of the solubility of the cellulose in this solvent). The main relaxation of the material is successfully modeled through the quasi-point defects theory developed by Perez et al. [12]. Although more experiments (perhaps not technically possible) would be necessary to achieve a more accurate modeling, the analysis of the different calculated parameters gives an estimation of the elementary movements (β) governing the mechanical behavior of these solutions in the glass transition domain. It suggests that the α relaxation observed corresponds to hierarchically correlated elementary movements of cellulose chains though the small concentration of the latter. One explanation might be the important stiffness of cellulose chains and their strong interactions with the solvent.

The isochronal and isothermal master curves obtained in this paper complete those reported in the previous work [4], thus providing the overall viscoelastic behavior of the solution from the liquid state to the solid state. This is of main interest for a process, the dissolution of cellulose in NMMO, which is an alternative to the viscose process.

References

[1] Turbak AF, Hammer RB, Davies RE, Hergert HL. Chemtec 1980;51:7.
[2] Courtaulds PLC. Polymer solutions, European Patent No. 83901828.0, 1983.
[3] Gagnaire D, Mancier D, Vincendon M. J Polym Sci Part A1: Polym Chem 1980;18:13.
[4] Blachot J-F, Brunet N, Cavaillé J-Y, Navard P. Rheol Acta 1998;37:107.
[5] Cavaillé J-Y, Salvia M, Merzeau P. Spectra 2000 1988;16:37.
[6] Ferry JD. Viscoelastic properties of polymers. 3rd ed. New York: Wiley, 1980. 641 pp.
[7] Williams ML, Landel RF, Ferry JD. J Am Chem Soc 1955;77:3701.
[8] Simatos D, Blond G. In: Blanchard JMV, Lillford PJ, editors. Nottingham: Nottingham University Press, 1994.
[9] Montes H, Mazeau K, Cavaillé J-Y. Macromolecules 1997;30:6977.
[10] Nowick AS, Berry BS. IBM J Res Dev 1961;5:297.
[11] Nowick AS, Berry BS. IBM J Res Dev 1961;5:312.
[12] Perez J. Physics and mechanics of amorphous polymers. Rotterdam, The Netherlands: Balkema, 1998 (see also the French Edition, Physique et mécanique des polymères amorphes, Ed. Technique et documentation, Lavoisier, Paris, 1992).
[13] Quinson R, Perez J, Germain Y, Murraciole J-M. Polymer 1995;36:743.
[14] Chazeau L, Paillet M, Cavaillé J-Y. J Polym Sci Part B: Polym Phys 1999;37:2151.
[15] Cavaillé J.-Y. Thèse d'état, INSA-Lyon, 1987.
[16] Cavaillé J-Y, Perez J, Johari GP. Phys Rev B 1989;39:2411.
[17] Cavaillé J-Y, Perez J, Johari GP. J Non–Cryst Solids 1991;131:935.
[18] Muzeau E, Vigier G, Vassoille R, Perez J. Polymer 1995;36(3):611.
[19] Flores R, Perez J, Cassagnau P, Michel A, Cavaillé J-Y. J Appl Polym Sci 1996;60:1439.
[20] Chabert E, Gauthier C, Perez J, submitted for publication.
[21] Gauthier C, Pelletier J-M, David L, Vigier G, Perez JJ. Non-Cryst Solids 2000;274:181.
[22] Starkweather HW. Polymer 1991;32(13):2443.
[23] Chazeau L, Cavaillé J-Y, Terech P. Polymer 1999;40(19):5333.